





Open Archive Toulouse Archive Ouverte

OATAO is an open access repository that collects the work of Toulouse researchers and makes it freely available over the web where possible

This is an author's version published in: <http://oatao.univ-toulouse.fr/21349>

Official URL: <https://doi.org/10.1016/j.aquatox.2018.11.020>

To cite this version:

Barrick, Andrew and Manier, Nicolas and Lonchambon, Pierre  and Flahaut, Emmanuel  and Jrad, Nisrine and Mouneyrac, Catherine and Châtel, Amélie *Investigating a transcriptomic approach on marine mussel hemocytes exposed to carbon nanofibers: An in vitro/in vivo comparison.* (2019) *Aquatic Toxicology*, 207. 19-28. ISSN 0166-445X

Any correspondence concerning this service should be sent to the repository administrator: tech-oatao@listes-diff.inp-toulouse.fr

1 **-Investigating a Transcriptomic Approach on Marine Mussel Hemocytes Exposed to Carbon**
2 **Nanofibers: an *in vitro/in vivo* Comparison**

3 Andrew Barrick^{1*}, Nicolas Manier², Pierre Lonchambon³, Emmanuel Flahaut³, Nisrine Jrad⁴,
4 Catherine Mouneyrac¹ and Amélie Châtel¹

5 1 : UBL (Université Bretagne et Loire), Mer Molécules Santé (MMS), Université Catholique de
6 l'Ouest, 3 place André Leroy, BP10808, 49008 Angers Cedex 01, France.

7 2: INERIS (Institut National de l'Environnement Industriel et des Risques),\ Expertise and assay
8 in ecotoxicology unit, Parc Technologique ALATA, 60550 Verneuil-en-Halatte, France.

9 3 :CIRIMAT, Université de Toulouse, CNRS, INPT, UPS, UMR CNRS-UPS-INP N°5085,
10 Université Toulouse 3 Paul Sabatier, Bât. CIRIMAT, 118, route de Narbonne, 31062 Toulouse
11 cedex 9, France

12 4 : LARIS (Laboratoire Angevin de Recherche en Ingénierie des Systèmes), EA-7315, Université
13 Catholique de l'Ouest - 3 place André Leroy, BP10808, 49008 Angers Cedex 01, France.

14 E-mail contact: andrew.barrick@etud.uco.fr

15

16

17

18 Key Words: Carbon nanofibers, Transcriptomics, *in vitro/in vivo* exposure, *Mytilus edulis*
19 Hemocytes

20 **Abstract**

21 Manufactured nanomaterials are an ideal test case of the precautionary principle due to their
22 novelty and potential environmental release. In the context of regulation, it is difficult to
23 implement for manufactured nanomaterials as current testing paradigms identify risk late into the
24 production process, slowing down innovation and increasing costs. One proposed concept, namely
25 safe(r)-by-design, is to incorporate risk and hazard assessment into the design process of novel
26 manufactured nanomaterials by identifying risks early. When investigating the manufacturing
27 process for nanomaterials, differences between products will be very similar along key
28 physicochemical properties and biological endpoints at the individual level may not be sensitive
29 enough to detect differences whereas lower levels of biological organization may be able to detect
30 these variations. In this sense, the present study used a transcriptomic approach on *Mytilus edulis*
31 hemocytes following an *in vitro* and *in vivo* exposure to three carbon nanofibers created using
32 different production methods. Integrative modeling was used to identify if gene expression could
33 be in linked to physicochemical features. The results suggested that gene expression was more
34 strongly associated with the carbon structure of the nanofibers than chemical purity. With respect
35 to the *in vitro/in vivo* relationship, results suggested an inverse relationship in how the
36 physicochemical impact gene expression.

37

38

39

40

41

42 **1. Introduction**

43 The assessment of environmental risk of manufactured nanomaterials (MNMs), or
44 nanomaterials designed for a specific purpose, in the marine environment is more of a hypothesis
45 than an established risk (Matranga and Corsi, 2012). Ecosystems are also influenced by multiple
46 stressors (e.g. urban and industrial runoff) often from nonpoint sources limiting the ability to prove
47 that MNMs pose significant risks. To assess the potential environmental risk of emerging
48 contaminants, environmental programs, like the European Water Framework Directive (WFD)
49 which follows the precautionary principle, aim to focus on prevention rather than mitigation. In
50 this sense, hazard assessment aims to identify the associated environmental impact with MNMs
51 prior to their use and, in some cases, eventual release into the environment (Canesi et al., 2008a).
52 In the context of regulation, it is difficult to implement this approach as current testing paradigms
53 identify risk late into the production process, slowing down innovation and increasing costs. To
54 address this, one of the proposed approaches, safe(r)-by-design (SbD), aims to incorporate hazard
55 assessment into the design process of novel MNMs(Schwarz-plaschg et al., 2017). The application
56 of SbD to MNMs was developed in the European FP7 projects NANoREG and Prosafe and is
57 being expanded on in the European Horizon 2020 project NanoReg2. The objectives of an SbD
58 approach is to apply the precautionary principle early in the production/innovation process and in
59 this way, hazards and risks can be identified early and strategies to mitigate their effects without
60 placing significant burdens for industry(Kraegeloh et al., 2018). It is important to note however
61 that the aim of SbD is not to completely remove the risk but to find ways to lower the risk without
62 hindering the performance of the product.

63 To adequately implement a SbD approach, rapid and cost-effective techniques need to be
64 developed to quickly screen the potential hazards of products. Testing that focuses on sub-
65 individual multi-endpoint responses may provide an ideal starting point for developing a rapid
66 prescreening strategy for MNMs (Moore, 2006). In the context of SbD, MNMs produced by a
67 company are also likely to have minimal differences which may make individual endpoints (e.g.
68 growth, mortality...) unsuitable in accurately detecting differences in the potential adverse effects
69 between MNMs. As a result, testing at lower levels (e.g. molecular or biochemical) of biological
70 organization may be more appropriate in discriminating between MNMs that are similar along
71 many key physicochemical properties. Due to the rapid rate that new nanomaterials are being
72 produced, as well as legislative and public concerns over the ethics of animal testing promoting
73 the use of the 3 R's (Replacement, Reduction and Refinement), *in vitro* testing that can be adapted
74 to a high throughput screening (HTS) approach can provide a relatively low cost means of
75 screening a large number of chemical in a short amount of time (Barrick et al., 2017). One of the
76 challenges however, is that *in vitro* testing has not been adequately demonstrated to date to be a
77 suitable alternative to *in vivo* testing for marine environmental risk assessment.

78 Transcriptomic tools could be considered as a suitable "HTS approach" for ecotoxicity as
79 it allows for an improved understanding of the molecular mechanisms underlying responses to
80 environmental contaminants and can screen a large number of endpoints in a short amount of time
81 (Snape et al., 2004). However, it is important to note that for marine species there is limited
82 knowledge for genes, limiting the number of available endpoints for testing (Revel et al., 2017).
83 Transcriptomics could also provide knowledge on mode of actions (MoAs) for MNMs and
84 represent a way to predict toxicity before stronger effects occur at higher levels of biological

85 organization (Revel et al., 2017). In the context of integrating ecotoxicological hazards into aSbD
86 approach, this is could be ideal in discriminating between similar products.

87 In this sense, the present study implemented a transcriptomic approach through real-time
88 quantitative PCR (qPCR) on a primary cell culture of *M. edulis* hemocytes to measure the
89 ecotoxicity of 3 carbon nanofibers (CNFs), GANF, GATam and GANFg, under development by
90 an industrial partner. The objectives of the study were i) to identify the impact of these products
91 on gene expression, ii) identify if the CNFs could be discriminated from one another through gene
92 expression, and iii) if *in vitro* testing could be considered a suitable alternative testing strategy. To
93 determine if the *in vitro* exposure could adequately be used as an alternative testing strategy, an *in*
94 *vivo* exposure was also conducted for comparison. The aim was not to have equivalent values
95 between *in vitro* and *in vivo* testing but to determine if both testing strategies developed the same
96 conclusions. After a 24-hour exposure, expression levels of a battery of genes implicated in
97 xenobiotic transport/transformation, oxidative stress, metabolic activity, cell transport,
98 cytoskeleton and cell cycle control were investigated. These endpoints were selected have been
99 used previously in to investigate the effects of nanomaterials on gene expression in *M. edulis*
100 (Châtel et al., 2018). The 24-hour exposure was selected as previous studies have shown this to be
101 the optimal duration to maintain *Mytilus* hemocytes in cell culture and previous study have shown
102 hemocytes, *in vitro* and *in vivo*, to respond to MNMs during this time period (Barrick et al., 2018;
103 Canesi et al., 2008b; Gagné et al., 2008; Katsumiti et al., 2014).

104 **2. Material and Methods**

105 ***2.1 Nanomaterials used in the study***

106 Three CNFs (GANF, GATam and GANFg) were provided by Grupo Antolin. The
107 CNFs are an industrial grade product for commercial use in automobile parts. Grupo Antolin
108 initially produced GANF through catalytic vapor deposition (CVD) using a natural gas and sulfur
109 feed stock at temperatures greater than 1100°C in a floating catalyst reactor (Vera-Agullo et al.,
110 2007; Weisenberger et al., 2009). Deposition of graphene layers is promoted by metallic nickel
111 while catalytically inactive NiS allows for the formation of helical-ribbons with a stacked cup
112 structure. To scale up production, a new method was developed to produce higher volumes of
113 CNFs. This is the process used to create GATam, which has slight differences in physicochemical
114 properties when compared to GANF. GANFg CNFs are created by super heating GANF at
115 2500°C, which decreases the interlayer spacing in the CNF and removes Nickel and Sulfur
116 impurities (Weisenberger et al., 2009). Physicochemical differences measured by Grupo Antolin
117 are summarized in table 1.

118 ***2.2 Preparation and characterization of nanomaterials***

119 Nanomaterial suspensions were prepared following the NANoREG Standard Operating
120 Procedure (SOP) (Jensen et al., 2011). Briefly, 15.36mg of nanomaterial powder was measured
121 into a 20mL Scint-Burk glass vial (WHEA989581; Wheaton Industries Inc.) which is prewet with
122 30µL of absolute ethanol. The volume was adjusted to 6mL with 0.05% Bovine Serum Albumin
123 (BSA)-water (w/v) to achieve a final concentration of 2.56mg/mL. The suspension was then placed
124 in an ice-water bath solution and sonicated using a Branson-S450 sonicator at 10% amplitude for
125 16 minutes. The suspension was left on ice for 10 minutes prior to use.

126 To characterize the ENM behavior, suspensions were diluted to 25.6mg/L in BSA stock
127 suspension, cell culture media and in 30 p.s.u. (practical salt units) of artificial sea water (ASW),

128 Tropic Marine, in 20mL Scint-Burk glass vials and maintained at test conditions. This
129 concentration was selected as it was found to achieve reliable results. Dynamic light scattering
130 (DLS) and zeta potential (Malvern ZS90) was measured at 0, 2, 4, 6 and 24 hours for each
131 suspension to characterize the behavior of the nanomaterials over the duration of the experiment.
132 Due to high ionic strength, zeta potential could not reliably be measured in cell culture media and
133 ASW.

134 Transmission Electron Microscopy (TEM) was also used for each suspension to
135 characterize the relative particle sizes of the ENMs. TEM (JEOL JEM 1400 plus @120kV, Japan)
136 was used to visualize morphology of CNFs in the stock suspensions, culture media and artificial
137 sea water. Carbon-coated grids were hydrophilized using a glow discharge apparatus (K100X,
138 Emitech, UK). The glow discharge was performed for 180 s at an air pressure of 10^{-1} mbar and an
139 electric current of 40 mA. This treatment was applied to TEM grids prior to the suspension
140 deposition as it prevents most of the artefactual agglomeration phenomenon during the drying of
141 the suspensions on the TEM grids (Dubochet et al., 1982).

142 CNFs suspensions were also analyzed using a Tecan Sunrise spectrometer to measure
143 optical density as an approximation of stability over the duration of the experiment . Each
144 suspension was measured across the visible light wavelength to determine which wavelength
145 yielded the highest value. It was identified that a 340nm wavelength yielded the highest
146 absorbance values for all three CNFS. 60 μ L of suspension was taken from the surface of the
147 liquids and triplicates were measured using a 96-well plate for all time points. The results were
148 then normalized using a blank for each media suspension and values at each time point were
149 adjusted relative to the start of the experiment.

150 Raman spectroscopy was performed using a confocal Jobin Yvon LABRAM HR800
151 spectrometer (red laser at 633 nm) using a maximum power of 5 mW with a spot size of *ca.* 1 μm .
152 Ten accumulations of 5s were acquired. Irradiation of the samples started 30s before acquisition
153 to limit the possible interference with fluorescence. 5 spectrums were obtained in 5 different areas
154 of each sample.

155

156 ***2.3 Hemocyte collection and establishment of primary cell culture***

157 *M. edulis* individuals of the same size ($4.2 \pm 0.23\text{cm}$) were collected from a relatively clean
158 sight, Saint-Cast-le-Guildo ($48^{\circ}37'48''\text{N}$ $2^{\circ}15'24''\text{W}$), previously identified as suitable for
159 experimental research (Chevé et al., 2014). Sampling was conducted in late fall to avoid the
160 reproductive period, which would potentially influence results. Mussels were placed in artificial
161 sea water (30 psu, at 15°C with a 12-hour light/day cycle) for a 2-day acclimation period prior to
162 testing.

163 A primary cell culture on *M. edulis* hemocytes was established following the methodology
164 described in (Barrick et al., 2018). A 23-gauge, 2mL syringe containing 0.1mL of Alseve (ALS)
165 buffer (20.8 g.L^{-1} glucose, 8 g.L^{-1} sodium citrate, 3.36 g.L^{-1} EDTA, 22.5 g.L^{-1} NaCl, pH 7.0) was
166 used to extract the hemolymph (Cao et al., 2003). After aspirating hemolymph from 5 organisms,
167 the needle was removed from the syringe and the contents were filtered through a $70\mu\text{m}$ filter into
168 a falcon tube maintained at 4°C . After extracting hemolymph from 40 mussels the total volume
169 was recorded.

170 Cell viability and cell concentration was then recorded through trypan blue exclusion.
171 Hemocyte concentration was diluted to $1 \times 10^6\text{ cells.mL}^{-1}$ using the ALS solution. $200\mu\text{L}$ of

172 hemolymph was then seeded into a 96-well microplate (2×10^5 cells/well). The plate was then
173 placed into an incubator at 18°C for 30 minutes, 3.5% CO_2 . After 30 minutes, hemolymph was
174 aspirated and replaced with adjusted Leibovitz L-15 medium ($20.2 \text{ g.L}^{-1}\text{NaCl}$, $0.54 \text{ g.L}^{-1}\text{KCl}$, 0.6
175 $\text{g.L}^{-1} \text{CaCl}_2$, $1 \text{ g.L}^{-1} \text{MgSO}_4$, $3.9 \text{ g.L}^{-1} \text{MgCl}_2$, $100 \text{ units.mL}^{-1}$ penicillin G, $100 \mu\text{g.mL}^{-1}$
176 streptomycin, 1% gentamycin, 10% glucose and 10% Fetal Bovine Serum (FBS), pH 7.0). Cells
177 were left to adhere overnight prior to exposure.

178 ***2.4 In vitro exposure***

179 Cell quality and attachment was visually confirmed the next day prior to ENM exposure
180 using an inverted confocal microscope. Cell culture media was then refreshed with cell culture
181 media containing ENMs in suspension (0.01 , 0.1 and 1 mg.L^{-1}) with three replicates per test
182 concentration. These concentrations were selected as they are within the range of previous test
183 concentrations used with *Mytilus* hemocytes (Canesi et al., 2008b). The cell culture was then
184 returned to the incubator for 24 hours. After 24 hours, the media was removed and the cells were
185 washed twice with PBS ($1,100 \text{ mOSM}$). $50 \mu\text{L}$ of trypsin was then added for to each well to detach
186 the cells. After 5 minutes, detachment was confirmed using an inverted confocal microscope after
187 gently mixing the solution with a $20 \mu\text{L}$ pipette. $150 \mu\text{L}$ of cell culture media containing 10% FBS
188 was then added to arrest trypsin activity. The cells were then collected in an Eppendorf tube and
189 centrifuged at $500g$ for 5 minutes at 4°C to pellet the cells. Cell culture media was removed and
190 the cells were washed with PBS ($1,100 \text{ mOsm}$). This step was repeated twice, after which the cell
191 pellet was stored at -80°C prior to analysis.

192 ***2.5 In vivo exposure***

193 60 Mussels were placed in four 12L aquariums (1.25 mussels.L⁻¹) and maintained in the same
194 conditions as the acclimation period. ENMs were spiked once into each aquarium at the three test
195 concentrations (0.01, 0.1 and 1mg.L⁻¹) with 15 organisms per test concentration. Organisms were
196 exposed for 24 hours, unfed and oxygenated using a glass Pasteur pipette, after which hemolymph
197 was pooled for each test concentration following the previously described method.

198 **2.6 qPCR assay**

199 *2.6.1 RNA extraction*

200 RNA extraction was conducted using a previously defined protocol (Châtel et al., 2018).
201 Briefly, the hemocytes were ground in TRIzol Reagent® (Ref: 15596026, Invitrogen™) 1ml per
202 100 mg of cells. Centrifugation (12000g for 10 minutes at 4°C) was then used to suppress cellular
203 debris. 0.2 mL Chloroform per 1mL of TRIzol was added to the supernatant and shaken vigorously
204 prior to centrifugation (12000 g for 15 minutes at 4°C) to ensure a phase separation with the clear
205 upper aqueous phase, containing RNA, being collected. 0.5 mL of isopropanol per ml of TRIzol
206 Reagent® was then added and the solution was incubated for 10 minutes at room temperature, to
207 precipitate the RNA. Centrifugation (12000g for 10 minutes at 4°C) was then used to the pellet
208 RNA. The pellet was washed with 200µL of absolute ethanol and the RNA was then pellet again
209 through centrifugation (12000g for 5 minutes at 4°C). The ethanol was then evaporated and the
210 pellet was allowed to completely dry under a flow hood before adding 10µL of Diethyl
211 pyrocarbonate (DEPC) water.

212 *2.6.2 Determination of total RNA and preparation of cDNA*

213 Determination of total RNA of each extraction was carried out with a Nanodrop using 1µL
214 of RNA per sample (Thermo Scientific™ NanoDrop 2000). First strand cDNA synthesis was

215 conducted using 0.2 µg of RNA extractand was mixed with oligo-dT primers following the
216 SuperScript™ III First-Strand Synthesis SuperMix protocol supplied by Invitrogen™.

217 *2.6.3 qRT-PCR analysis*

218 cDNA amplification was performed using a LightCycler 480 Real Time PCR system
219 (Biorad) using SYBR Green Power Master Mix (Invitrogen) with specific primer pairs (see
220 supplemental material). Thermocycling was conducted using polymerase activation at 94°C for 2
221 minutes with an amplification and quantification cycle repeated for 50 cycles (94°C for 30 seconds,
222 58°C for 30 seconds, 72°C 30 seconds). The cq (Threshold cycle) values were recorded for analysis
223 using actin as a housekeeper gene. Each gene was analyzed in triplicate.

224 *2.6.4 Statistical analysis and modelling*

225 Statistical Analysis was conducted using “R Studio 3.3.1”(R Studio Team, 2015). The
226 measured values were compared among the different groups using nonparametric analysis through
227 Kruskal-Wallis and Dunn’s analysis (R package dunn.test) with a $P < 0.05$ indicating statistical
228 significance. P-values were then corrected using false discovery rate (fdr) using the R-package
229 hmisc. To create an integrative analysis, partial least square discriminant analysis (PLS-DA) was
230 used to determine if test conditions could be discriminated from the control(Bertrand et al., 2017;
231 Cho et al., 2008). PLS-DA was selected as it has good performance when dealing with multi-
232 collinear data with small samples and many variables (genes). ENMs and test condition (*in vitro*
233 or *in vivo*) were analyzed separately to identify which genes were significantly impacted by the
234 exposure conditions used. Variable Importance on Projection (VIP) was scored to identify which
235 genes were most important in group discrimination (Jaumot et al., 2015). For each CNF, both *in*
236 *vitro* and *in vivo* exposures were plotted together. For each test condition, a correlation circle was

237 plotted on the factorial plane combining the first two axes of the PLS-DA model. Vectors of the
238 correlation circle represent the variables (genes) used to generate the model. Vectors describe the
239 relationships between the genes and each of the axes.

240 To identify if production process influenced ecotoxicity, results were analyzed to
241 determine if product features could be linked to gene expression. As the CNF products were
242 similar in all aspects except for small differences due to the production process, the focus of the
243 analysis was to determine if these differences could be linked to gene expression results. Two
244 analyses of correlation were conducted to *i*)determine if gene expression could be correlated with
245 the I_D/I_G -band ratio from Raman spectroscopy and *ii*)determine if there is a relationship between
246 the reported purity of the CNFs. To achieve this, foreach test condition (*in vitro* or *in vivo*) results
247 were separated based on test concentration (0.01, 0.1 and 1 mg.L⁻¹). Using these groups, Pearson's
248 correlation coefficient was used to define their relationship between I_D/I_G ratio and chemical purity
249 with gene expressions. Each gene was analyzed at each test concentration to determine statistical
250 significance using at $P < 0.05$.

251

252 **3. Results**

253 *3.1 Physicochemical characterization*

254 TEM results indicated that aggregation/agglomeration occurred in all media but no clear
255 differences between suspensions could be identified (Figures 1a-i). TEM results for ASW media
256 were difficult to analyze due to deposition of salt during the grid preparation. Raman spectroscopy
257 results indicated that the ratio between the Dband and Gband (I_D/I_G) could be used to discriminate
258 between the CNFs. GANF had a higher I_D/I_G -band ratio (1.26) than GATam (1.07) and

259 GANFg(0.78) indicating that GANF has the highest number of structural defects and GANFg has
260 the lowest number of structural defects (Figure 2a-c).

261 All suspensions could be analyzed through DLS with results being considered good quality
262 (Table 2). Stock suspensions for GANF (489.3 d-nm), GATam (414.3 d-nm) and GANFg (479.8
263 d-nm) were all comparable in the size of agglomerates. When prepared in culture media, GANF
264 (260.1 d-nm), GATam (197.8 d-nm), and GANFg (244.1 d-nm) were still comparable in e but
265 agglomerate sizes were notably smaller than the stock suspensions. This was also observed in
266 ASW where GANF (186.7 d-nm), GATam (223 d-nm) and GANFg (217.4 d-nm) agglomerates
267 were smaller in size when compared to the stock media but were similar in size to the
268 measurements obtained in the cell culture media. The size of agglomerates after 24 hours were
269 similar to the start of the experiment for all test media.

270 The optical density measured in the stock suspension suggested that CNFs remaining in
271 suspension were similar between GANF (11.5%) and GATam (17.62%) in the stock suspensions
272 whereas GANFg was higher (47.72%), suggesting more CNFs remained in suspension (Figure 3).
273 Optical density in cell culture media for GANF (47.88%), GATam (86.34%) and GANFg
274 (89.80%) was notably increased when compared to the stock suspension. For suspensions prepared
275 in ASW, GANF (40.67%) and GATam (77.79%) where similar in optical density to the cell culture
276 media. GANFg (40.67%) had lower optical density in ASW.

277 *3.2 Gene expression Analysis*

278 *3.2.1 in vivo*

279 Mussels exposed to the CNFs showed limited statistical significant between the control
280 and the test concentrations for many of the genes suggesting little effects when exposed to the
281 CNFs (Table 3). Histograms associated with the results can be found in the supplemental material.

282 3.2.1.1 *Oxidative stress/detoxification*

283 SOD mRNA levels were not significantly impacted. Catalase gene was significantly
284 increased when exposed to GANF (0.01 and 1 mg.L⁻¹) and GATam (0.01mg/L). . HSP70 was also
285 not significantly increased when exposed to GANF (0.01 mg.L⁻¹). GST was significantly increased
286 by GATam (1mg.L⁻¹). Cytochrome P450 was significantly MT was significantly increased when
287 exposed to GANFg (0.1 and 1mg.L⁻¹).

288 3.2.1.2 *Cytoskeleton, Cell metabolism & Cell Cycle Control*

289 B-tub was not significantly impacted. MRP was significantly decreased by GATam (0.01 and
290 1mg.L⁻¹) and GANFg (1mg.L⁻¹). Na/K ATPase was not significantly impacted. P53 was
291 significantly decreased by GANF (0.01 and 1mg.L⁻¹). Lysozyme gene expression was not
292 significantly impacted.

293 3.2.2 *in vitro*

294 Mussels exposed to the CNFs showed statistical significance with the *in vitro* exposure to
295 all three CNFs with more significant effects occurring than with the *in vivo* exposure (Table 4).
296 Histograms associated with the results can be found in the supplemental material.

297 3.2.2.1 *Oxidative stress/detoxification*

298 SOD mRNA levels were significantly decreased when mussels were exposed to GANF
299 (1mg.L⁻¹), GATam (0.01 and 0.1 mg.L⁻¹) and GANFg (0.01 and 0.1mg.L⁻¹). Catalase gene had no

300 significant effects. HSP70 was also significantly increase for GANF (0.01 and 1mg.L⁻¹), GATAM
301 (0.1 and 1mg.L⁻¹) and GANFg (0.01 and 1mg.L⁻¹). GST was significantly increased by GANF
302 (0.1 and 1mg.L⁻¹), GATam (0.1mg.L⁻¹) and GANFg (0.01 and 1 mg.L⁻¹). Cytochrome P450 was
303 not statistically significant. MT was significantly increased when exposed to GANF (0.1 and
304 1mg.L⁻¹), GATAM (1mg.L⁻¹) and GANFg (0.01 and 1mg.L⁻¹).

305 3.2.2.2 Cytoskeleton, Cell metabolism & Cell Cycle Control

306 B-tub was significantly decreased when exposed to GANF (0.1 and 1mg.L⁻¹), GATam
307 (0.01 and 0.1mg.L⁻¹) and GANFg (1mg.L⁻¹). PgP was only significantly affected by GANF
308 (1mg.L⁻¹). MRP was only affected by GATam (0.01mg.L⁻¹). Na/K ATPase was only significantly
309 affected by GANF (0.1 and 1mg.L⁻¹) and GATam (0.1 and 1 mg.L⁻¹). P53 was significantly
310 increased by GATam (0.01mg.L⁻¹). ATP synthase was significantly increased by GATam (1mg.L⁻¹)
311 and significant decreased by GANFg(0.01 and 1 mg.L⁻¹). Lysozyme gene expression was not
312 significantly impacted.

313 3.3 PLS-DA analysis

314 VIP values were identified for all 6 conditions and summarized in the table 5. When
315 analyzing the *in vivo* and *in vitro* exposure conditions most of the genes were identified as
316 important in describing variation between test conditions (>0.8). Of the genes used, consistently
317 high VIP values were found with ATP synthase, P53, metallothionein, lysozyme, catalase and
318 superoxide dismutase indicating these genes were essential in discriminating between test
319 concentrations. The results of the model were then plotted on a factorial plane describing the
320 relationship between genes (Figure 4). This was then used to plot the test conditions of each CNF

321 with their orientation dependent on which genes more effectively described the test condition
322 (Figure 5).

323 PLS-DA analysis for GANF *in vivo* showed that 0.01mg.L⁻¹ and 1mg.L⁻¹ test
324 concentrations were be discriminated from the control and showed a high degree of separation
325 (Figure 5A). 0.1 mg.L⁻¹ could be discriminated from the control but was similar in gene expression.
326 When analyzing the PLS-DA model for GANF *in vitro* results showed that all three test
327 concentrations could be discriminated from the control and showed a high degree of separation
328 between concentrations. 0.01 and 0.1 mg.L⁻¹ exposure times were similar in response. For both *in*
329 *vivo* and *in vitro* results the 1mg.L⁻¹ test concentration was clearly separated.

330 The PLS-DA model for GATam *in vivo* results also showed discrimination from the control
331 at 0.01, 0.1mg.L⁻¹ and at 1mg.L⁻¹ (Figure 5B). This pattern was observed as well for the *in vitro*
332 test condition but little similarities were observed between the two test conditions.

333 The PLS-DA model GANFg *in vivo* had a clear separation of the test concentrations from
334 the control (Figure 5C). GANFg *in vitro* showed clear separation from the control for all three test
335 concentrations and 0.01mg.L⁻¹ and 1mg.L⁻¹ exposure conditions were similar in response.

336 3.4 Correlating CNF form with gene expression

337 To determine if relationships between gene expression and differences in the CNF
338 production process could be established Pearson's correlation coefficient and CNF structural
339 purity (as measured through Raman spectrometry) was used. Positive correlations would indicate
340 that as the I_D/I_G-band ratio increases, gene expression increases where as a negative correlation
341 would result in an inverse interpretation. Significant positive correlations in the relationship

342 between gene expression and CNF purity would imply that as purity increases, gene expression
343 increases. A negative correlation would suggest that as purity decreases, gene expression increases.

344 When test concentrations were controlled for strong correlations between gene expression
345 and I_D/I_G-band ratio could be identified (Table 6). For the *in vivo* exposure there were clear
346 differences with test concentration and relationship I_D/I_G-band ratio. At a concentration of 0.01
347 mg.L⁻¹ HSP70, GST, SOD, ATP synthase and B-tubulin gene expressions had strong positive
348 correlations with the I_D/I_G-band ratio where at a dose of 0.1 mg.L⁻¹ only MRP gene had a significant
349 correlation. For mussels exposed to 1mg.L⁻¹, metallothionein, lysozyme, PgP, ATP synthase, P53
350 and MRP gene expression levels had all positive correlations. However, mussels exposed *in vitro*
351 to 0.01mg.L⁻¹, showed that HSP70, GST, metallothionein and ATP synthase mRNA levels had
352 significant negative correlations with the I_D/I_G-band ratio where Na/K ATPase and MRP genes
353 had significant positive correlations. At a concentration of 0.1 mg.L⁻¹, SOD, lysozyme, PgP and
354 cytochromeP450 gene expression levels had negative correlations and GST, Na/K ATPase and
355 P53 genes had positive correlations. At a concentration of 1mg.L⁻¹, SOD, lysozyme,
356 cytochromeP450 and ATP synthase mRNA levels had strong positive correlations.

357 When determining the relationship between gene expression and CNF chemical purity (as
358 reported in Table 1), there were some significant relationships were identified but there were less
359 correlations than when comparing gene expression to the D/G band ratio (Table 7). When looking
360 at the *in vivo* exposure condition, β-tubulin, Na/K ATPase and P53 genes had significant negative
361 correlations with purity of the CNF at 0.01 mg.L⁻¹. At 0.1 mg.L⁻¹ exposure condition, HSP70,
362 GST, SOD, β-tubulin and MRP mRNA expressions depicted significant negative correlations with
363 purity whereas catalase gene had a significant positive relationship. At 1mg.L⁻¹, only MRP showed
364 a significant negative correlation to the purity. For the *in vitro* exposure condition, PgP,

365 cytochromeP450 and Na/K ATPase mRNA levels had negative correlations whereas GST and P53
366 genes had positive correlations. At 1mg.L⁻¹, HSP70 and Na/K ATPase expressions had significant
367 negative relationships whereas GST and PgP mRNA levels had significant positive relationships
368 with purity of CNF.

369

370 **4. Discussion**

371 The aim of the study was to investigate whether or not differences in the production process
372 of CNFs would alter gene expression profiles as well as to establish an *in vitro/in vivo* comparison.
373 In this sense, the first objective was to establish if the three CNFs have similar physicochemical
374 and to determine differences between *in vitro* and *in vivo* stability and hydrodynamic diameters.

375 *4.1 Physico-chemical characterization*

376 To maintain a relevant comparison between the 3 CNFs, the physico-chemical properties
377 of the CNFs in suspensions need to be accounted for. In this sense, DLS is a commonly used
378 technique for measuring ENMs in suspension but it is limited in the sense that it assumes a
379 spherical shape for the particles. In the context of CNFs this does not hold true for the single fibers,
380 but agglomerates can be approximated as ovoid and the size of the particles can be approximated
381 (Reinert et al., 2015).The DLS results suggest that particle sizes are comparable between CNFs as
382 well as between *in vitro* and *in vivo* assays. In addition to this, the optical density results suggest
383 that the test suspensions are somewhat stable with slight differences between *in vitro* and *in vitro*
384 test media for GATam and GANF. As a result, the CNFs used in the study can be considered to
385 have similar physico-chemical properties between the two testing strategies, facilitating an *in*

386 *vitro/in vivo* comparison. It is however important note that differences between the media may
387 lead to differences in sedimentation and effectively change the dosimetry.

388 Another interesting observation is that the CNFs displayed poor stability in ultra-pure
389 water whereas in both culture media and ASW the stability was improved. One potential
390 explanation for this observation is that the ionic strength of these suspensions decreased the surface
391 potential of the CNFs, reducing rate at which particles interact with other another (Pavlin and
392 Bregar, 2012). This is interesting as it would imply that the behavior of the CNFs in the ocean will
393 be different than the behavior in fresh water ecosystem, which can lead to distinct differences in
394 toxicity profiles.

395 Of the methods used to characterize the CNFs in the present study, only Raman
396 spectroscopy demonstrated clear differences between the CNFs. The comparison of the Raman
397 spectra of the 3 samples illustrates the influence of the annealing treatment with a clear
398 improvement of the I_D/I_G intensity ratio, decreasing from 1.3 (Fig. 2(a)) to 0.8 (Fig. 2(c)) and
399 evidencing a significant improvement of the structure of the carbon network, also visible with the
400 increased intensity of the 2D band (2650 cm^{-1}). Sample GATam (Fig. 2(b)) lies in between with
401 an intermediate value of the I_D/I_G intensity ratio of 1.1 but a noisier spectrum, although all data
402 were acquired exactly in the same experimental conditions. All 3 samples exhibited some
403 fluorescence leading to an important background signal. For this reason, irradiation of the samples
404 started 30s before acquisition to limit this phenomenon. It is important to note that Raman
405 spectroscopy does not allow a direct measurement of the chemical purity of the samples but more
406 of the level of structural defects (Ivanova et al., 2012). In the context of SbD and the case study
407 this is important because the structural quality of the CNFs may impact the performance of the
408 products and GATam may be a more desirable product than GANF as a result. In the context of

409 ecotoxicological hazards structural defects can lead to the functionalization of CNFs, providing
410 favorable binding sites for ions or molecules, which can lead to differences in hazard profiles.

411 *4.2 Gene expression*

412 The endpoints used in the present study provides broad spectrum response analysis of
413 hemocyte gene expression to CNF exposure, which allows for characterization of mechanisms of
414 action. To the authors' best knowledge, this is the first time that carbon nanofibers have been
415 investigated for ecotoxicological effects on mussels. As a result, there are limited examples that
416 could be considered a suitable comparison. Of the information available mussel hemocytes,
417 exposed *in vitro* and *in vivo* for 24 hours, have been shown to display sublethal responses to carbon
418 black and fullerene (0.01-1mg.L⁻¹) with little to no effects when exposed to a carbon nanotube
419 (0.01-1mg.L⁻¹) (Canesi et al., 2010, 2008b; Moore et al., 2009). Previous studies in human
420 toxicology have shown induction of oxidative stress and inflammation when cells, IL-8, A549 and
421 HaCaT, were exposed to multi-walled carbon nanotubes at 1mg/L and 25mg.L⁻¹ for 24 hours
422 (Vitkina et al., 2016; Ye et al., 2009). When analyzing the *in vivo* responses, the gene expression
423 had little significant effects (which may be attributed to the small sample sizes) with all three CNFs
424 and little clear pattern is evident with the CNFs. There is however a notable trend for GATam to
425 have higher fold expressions which could suggest more adverse effects may occur with this CNF.

426 When looking at the *in vitro* exposure however, hemocytes showed more significant effects
427 when compared to the *in vivo* exposure for all CNFs with many of the gene response associated
428 with oxidative and xenobiotic stress. This can be attributed to the simpler exposure scenario for
429 the *in vitro* exposure as the cells are directly exposed to the CNFs. When looking at the results for
430 approximated stability, GANF showed the least stability of the three CNFs in culture media. This

431 observation could suggest that due to the a sedimentation effect the effective dosage for GANF is
432 higher than the other two CNFs (Deloid et al., 2017; Hinderliter et al., 2010). This could also
433 suggest that these CNFs are aggregating at the bottom of the well and not interacting with the cells,
434 which can complicate the comparison between the three CNFs. Looking at the gene expression
435 holistically more significant effects occur with GANFg at 0.01mg.L^{-1} which could suggest this
436 product is more hazardous. The results of the *in vitro* approach may suggest that all three CNFs
437 could potentially cause oxidative and xenobiotic stress, which is not in agreement with the *in vivo*
438 approach. It is also important to note that the cell culture is a complex media consisting of a mixture
439 of proteins, which can lead to protein corona that does not occur naturally. As a result, further
440 analysis of dosimetry may be necessary when applying an *in vitro* approach for SbD in order to
441 demonstrate it is an accurate predictor of *in vivo* effects.

442 4.3 PLS-DA analysis

443 The integrative analysis through PLS-DA showed some unexpected results in that almost
444 all of the genes were important in the discrimination between test concentrations for all the CNFs
445 and for both *in vivo* and *in vitro* test conditions, highlighting its sensitivity in identifying sublethal
446 effects. Of these genes however, ATP synthase, P53, metallothionein, PgP and HSP70 were
447 identified as the most important discriminators for almost all test conditions. This suggests that
448 exposure to the CNFs is influencing a wide array of cellular functions (oxidative stress,
449 detoxification, cytoskeleton, cellular metabolism and cell cycle control) which can alter cell
450 functioning and potentially cascade into higher levels of biological organization. When comparing
451 the VIP values *in vivo* to *in vitro* it became apparent that in general there were some similarities in
452 the values between the two testing conditions. However, when analyzing the correlation circles the
453 relationship between genes was not consistent between the *in vitro* and *in vivo* exposures. The *in*

454 *vivo/in vitro* relationship is a challenge to many investigators as gene responses are often not
455 consistent between the two testing strategies (Heise et al., 2012).

456 4.4 Correlation CNF properties to Gene expression

457 In the context of applying ecotoxicology to a SbD for MNMs, there needs to be an
458 identification of what features of MNMs cause toxicity. The CNFs used in the present study
459 provide an ideal case study for the application of SbD as the products are very similar which allow
460 for an analysis on how the differences in production influence ecotoxicity. In this sense, structural
461 purity, measured through the I_D/I_G-band ratio, and overall purity were identified as potential
462 discriminators between the CNFs. Of these two measurements, the relationship between the I_D/I_G-
463 band ratio proved to be more strongly correlated with gene expression than chemical purity of
464 CNF. *In vivo*, all the genes showed a positive correlation with the I_D/I_G-band ratio indicating that
465 gene expression increased with structural impurities. With the *in vitro* results however, the inverse
466 is observed in the fact that gene expression was more strongly correlated with a decrease in the
467 I_D/I_G-band ratio. A previous study investigating the physicochemical relationship between toxicity
468 and MWNCT was able to demonstrate that the presence of proteins profoundly affects their
469 behavior in media and could alter their toxicity as a result, which may explain the difference in
470 interpretation(Allegri et al., 2016). The relationship between test media properties and CNFs
471 behavior requires further investigation, in particular the role of a protein corona in gene expression.
472 This does however provide insight that could be useful in linking ecotoxicity results in a way that
473 can promote SbD strategies.

474

475 5. Conclusion

476 Transcriptomic is a promising emerging tool to implement ecotoxicology into a SbD
477 approach for MNMs. The results in the present study demonstrate a way in which gene expression
478 can be used to provide information to improve the safety of MNM products. In the context of the
479 current study the *in vitro* and *in vivo* tests were not consistent in their interpretation of which CNF
480 was “least safe”, suggesting that *in vitro* and *in vivo* strategies need to be investigated in parallel
481 to verify that an *in vitro* approach using *M. edulis* hemocytes is a suitable alternative testing
482 strategy. It is however important to note that while *in vitro/in vivo* extrapolation remains a
483 challenge requiring additional research, the application of ecotoxicology in SbD may require the
484 use of *in vitro* testing to adequately screen products produced by industry in a cost effective and
485 timely manner.

486

487 **Acknowledgements:** The research contained within this publication was funded by the European
488 Union’s Horizon 2020 research and innovation program NANoREG2 under grant agreement
489 646221.

490 "The sole responsibility of this publication lies with the author. The European Union is not
491 responsible for any use that may be made of the information contained therein."

492

493

494

495

496

497

498

499

500

501

502 **References**

- 503 Allegri, M., Perivoliotis, D.K., Bianchi, M.G., Chiu, M., Pagliaro, A., Koklioti, M.A., Trompeta,
504 A.F.A., Bergamaschi, E., Bussolati, O., Charitidis, C.A., 2016. Toxicity determinants of
505 multi-walled carbon nanotubes: The relationship between functionalization and
506 agglomeration. *Toxicol. Reports* 3, 230–243. <https://doi.org/10.1016/j.toxrep.2016.01.011>
- 507 Barrick, A., Châtel, A., Bruneau, M., Mouneyrac, C., 2017. The role of high-throughput
508 screening in ecotoxicology and engineered nanomaterials. *Environ. Toxicol. Chem.* 9999,
509 1–11. <https://doi.org/10.1002/etc.3811>
- 510 Barrick, A., Guillet, C., Mouneyrac, C., Châtel, A., 2018. Investigating the establishment of
511 primary cultures of hemocytes from *Mytilus edulis*. *Cytotechnology*.
512 <https://doi.org/10.1007/s10616-018-0212-x>
- 513 Bertrand, C., Devin, S., Mouneyrac, C., Giambérini, L., 2017. Eco-physiological responses to
514 salinity changes across the freshwater-marine continuum on two euryhaline bivalves:
515 *Corbicula fluminea* and *Scrobicularia plana*. *Ecol. Indic.* 74, 334–342.
516 <https://doi.org/10.1016/j.ecolind.2016.11.029>

517 Canesi, Ciacci, C., Vallotto, D., Gallo, G., Marcomini, A., Pojana, G., 2010. In vitro effects of
518 suspensions of selected nanoparticles (C60 fullerene, TiO₂, SiO₂) on *Mytilus* hemocytes.
519 *Aquat. Toxicol.* 96, 151–158. <https://doi.org/10.1016/j.aquatox.2009.10.017>

520 Canesi, L., Borghi, C., Ciacci, C., Fabbri, R., Lorusso, L.C., Vergani, L., Marcomini, A., Poiana,
521 G., 2008a. Short-term effects of environmentally relevant concentrations of EDC mixtures
522 on *Mytilus galloprovincialis* digestive gland. *Aquat. Toxicol.* 87, 272–279.
523 <https://doi.org/10.1016/j.aquatox.2008.02.007>

524 Canesi, L., Ciacci, C., Betti, M., Fabbri, R., Canonico, B., Fantinati, A., Marcomini, A., Pojana,
525 G., 2008b. Immunotoxicity of carbon black nanoparticles to blue mussel hemocytes.
526 *Environ. Int.* 34, 1114–1119. <https://doi.org/10.1016/j.envint.2008.04.002>

527 Cao, A., Mercado, L., Ramos-Martinez, J.I., Barcia, R., 2003. Primary cultures of hemocytes
528 from *Mytilus galloprovincialis* Lmk.: Expression of IL-2R α subunit. *Aquaculture* 216, 1–8.
529 [https://doi.org/10.1016/S0044-8486\(02\)00140-0](https://doi.org/10.1016/S0044-8486(02)00140-0)

530 Châtel, A., Lièvre, C., Barrick, A., Bruneau, M., Mouneyrac, C., 2018. Transcriptomic approach:
531 A promising tool for rapid screening nanomaterial-mediated toxicity in the marine bivalve
532 *Mytilus edulis* —Application to copper oxide nanoparticles. *Comp. Biochem. Physiol. Part*
533 *C Toxicol. Pharmacol.* 205, 26–33. <https://doi.org/10.1016/j.cbpc.2018.01.003>

534 Chevé, J., Bernard, G., Passelergue, S., Prigent, J.-L., 2014. Suivi bactériologique des gisements
535 naturels de coquillages de l’Ille-et-Vilaine et des Côtes- d’Armor fréquentés en pêche à pied
536 1–99.

537 Cho, H.-W., Kim, S.B., Jeong, M.K., Park, Y., Miller, N.G., Ziegler, T.R., Jones, D.P., 2008.

538 Discovery of metabolite features for the modelling and analysis of high-resolution NMR
539 spectra. *Int. J. Data Min. Bioinform.* 2, 176–92.

540 Deloid, G.M., Cohen, J.M., Pyrgiotakis, G., Demokritou, P., 2017. Preparation, characterization,
541 and in vitro dosimetry of dispersed, engineered nanomaterials. *Nat. Protoc.* 12, 355–371.
542 <https://doi.org/10.1038/nprot.2016.172>

543 Dubochet, J., Groom, M., Mueller-Neuteboom, S., 1982. The Mounting of Macromolecules for
544 Electron Microscopy with Particular Reference to Surface Phenomena and the Treatment of
545 Support Films by Glow Discharge. *Adv. Opt. Electron Microsc.* 8, 107–135.

546 Fenwick, N., Griffin, G., Gauthier, C., 2009. The welfare of animals used in science: How the
547 “Three Rs” ethic guides improvements. *Can. Vet. J.* 50, 523–30.

548 Gagné, F., Auclair, J., Turcotte, P., Fournier, M., Gagnon, C., Sauvé, S., Blaise, C., 2008.
549 Ecotoxicity of CdTe quantum dots to freshwater mussels: Impacts on immune system,
550 oxidative stress and genotoxicity. *Aquat. Toxicol.* 86, 333–340.
551 <https://doi.org/10.1016/j.aquatox.2007.11.013>

552 Heise, T., Schug, M., Storm, D., Ellinger-Ziegelbauer, H., J. Ahr, H., Hellwig, B., Rahnenführer,
553 J., Ghallab, A., Guenther, G., Sisnaiske, J., Reif, R., Godoy, P., Mielke, H., Gundert-Remy,
554 U., Lampen, A., Oberemm, A., G. Hengstler, J., 2012. In Vitro - In Vivo Correlation of
555 Gene Expression Alterations Induced by Liver Carcinogens. *Curr. Med. Chem.* 19, 1721–
556 1730. <https://doi.org/10.2174/092986712799945049>

557 Hinderliter, P.M., Minard, K.R., Orr, G., Chrisler, W.B., Thrall, B.D., Pounds, J.G., Teeguarden,
558 J.G., 2010. ISDD: A computational model of particle sedimentation, diffusion and target

559 cell dosimetry for in vitro toxicity studies. Part. Fibre Toxicol. 7, 36.
560 <https://doi.org/10.1186/1743-8977-7-36>

561 Ivanova, M. V., Lamprecht, C., Jimena Loureiro, M., Torin Huzil, J., Foldvari, M., 2012.
562 Pharmaceutical characterization of solid and dispersed carbon nanotubes as nanoexcipients.
563 Int. J. Nanomedicine 7, 403–415. <https://doi.org/10.2147/IJN.S27442>

564 Jaumot, J., Navarro, A., Faria, M., Barata, C., Tauler, R., Piña, B., 2015. qRT-PCR evaluation of
565 the transcriptional response of zebra mussel to heavy metals. BMC Genomics 16.
566 <https://doi.org/10.1186/s12864-015-1567-4>

567 Jensen, K.A., Kembouche, Y., Christiansen, E., E., J., N.R., W., Giot, C., Spalla, O., Witschger,
568 O., 2011. Final protocol for producing suitable manufactured nanomaterial exposure media.
569 NANoREG A common Eur. approach to Regul. Test. Nanomater. Web-Report.

570 Katsumiti, A., Berhanu, D., Howard, K.T., Arostegui, I., Oron, M., Reip, P., Valsami-Jones, E.,
571 Cajaraville, M.P., 2014. Cytotoxicity of TiO₂ nanoparticles to mussel hemocytes and gill
572 cells in vitro: Influence of synthesis method, crystalline structure, size and additive.
573 Nanotoxicology 5390, 1–11. <https://doi.org/10.3109/17435390.2014.952362>

574 Kraegeloh, A., Suarez-merino, B., Sluijters, T., Micheletti, C., 2018. Implementation of Safe-by-
575 Design for Nanomaterial Development and Safe Innovation : Why We Need a
576 Comprehensive Approach. <https://doi.org/10.3390/nano8040239>

577 Matranga, V., Corsi, I., 2012. Toxic effects of engineered nanoparticles in the marine
578 environment: Model organisms and molecular approaches. Mar. Environ. Res. 76, 32–40.
579 <https://doi.org/10.1016/j.marenvres.2012.01.006>

580 Moore, M.N., 2006. Do nanoparticles present ecotoxicological risks for the health of the aquatic
581 environment? *Environ. Int.* 32, 967–976. <https://doi.org/10.1016/j.envint.2006.06.014>

582 Moore, M.N., Readman, J.A.J., Readman, J.W., Lowe, D.M., Frickers, P.E., Beesley, A., 2009.
583 Lysosomal cytotoxicity of carbon nanoparticles in cells of the molluscan immune system:
584 An in vitro study. *Nanotoxicology* 3, 40–45. <https://doi.org/10.1080/17435390802593057>

585 Pavlin, M., Bregar, V.B., 2012. Stability of nanoparticle suspensions in different biologically
586 relevant media. *Dig. J. Nanomater. Biostructures* 7, 1389–1400.

587 R Studio Team, 2015. RStudio: Integrated Development for R.

588 Reinert, L., Zeiger, M., Suárez, S., Presser, V., Mücklich, F., 2015. Dispersion analysis of carbon
589 nanotubes, carbon onions, and nanodiamonds for their application as reinforcement phase in
590 nickel metal matrix composites. *RSC Adv.* 5, 95149–95159.
591 <https://doi.org/10.1039/C5RA14310A>

592 Revel, M., Châtel, A., Mouneyrac, C., 2017. Omics tools: New challenges in aquatic
593 nanotoxicology? *Aquat. Toxicol.* 193, 72–85. <https://doi.org/10.1016/j.aquatox.2017.10.005>

594 Schwarz-plaschg, C., Kallhoff, A., Eisenberger, I., 2017. Making Nanomaterials Safer by
595 Design ? 277–281.

596 Snape, J.R., Maund, S.J., Pickford, D.B., Hutchinson, T.H., 2004. Ecotoxicogenomics: The
597 challenge of integrating genomics into aquatic and terrestrial ecotoxicology. *Aquat.*
598 *Toxicol.* 67, 143–154. <https://doi.org/10.1016/j.aquatox.2003.11.011>

599 Vitkina, T.I., Yankova, V.I., Gvozdenko, T.A., Kuznetsov, V.L., Krasnikov, D. V., Nazarenko,
600 A. V., Chaika, V. V., Smagin, S. V., Tsatsakis, A.M., Engin, A.B., Karakitsios, S.P.,

601 Sarigiannis, D.A., Golokhvast, K.S., 2016. The impact of multi-walled carbon nanotubes
602 with different amount of metallic impurities on immunometabolic parameters in healthy
603 volunteers. *Food Chem. Toxicol.* 87, 138–147. <https://doi.org/10.1016/j.fct.2015.11.023>

604 Ye, S.F., Wu, Y.H., Hou, Z.Q., Zhang, Q.Q., 2009. ROS and NF- κ B are involved in upregulation
605 of IL-8 in A549 cells exposed to multi-walled carbon nanotubes. *Biochem. Biophys. Res.*
606 *Commun.* 379, 643–648. <https://doi.org/10.1016/j.bbrc.2008.12.137>

607

608

Measured property	Unit	GANF	GANFg	GATam
Fiber diameter (TEM)	nm	20-80	20-80	20-80
Carbon purity (TGA)	%	>85	>99	>80
Apparent density	g/cc	~0.06	~0.08	~0.08
Specific surface area (BET N ₂)	m ² /g	100-170	70-90	70-140
Graphitization degree (XRD)	%	~70	~90	~60
Electrical resistivity	Ω·m	1*10 ⁻³	1*10 ⁻⁴	1*10 ⁻³

Table 1: Physico-chemical properties reported by the industrial partner

Start of Experiment									
	Ganf			Gatam			Ganf		
	Z-average (d-nm)	Pdl	Zeta potential (mV)	Z-average (d-nm)	Pdl	Zeta potential (mV)	Z-average (d-nm)	Pdl	Zeta potential (mV)
Stock Suspension	489.3	0.128	-10.1	414.3	0.231	-13.8	479.8	0.178	-15.6
<i>M. edulis Culture Media</i>	260.1	0.359	-	197.8	0.272	-	244.1	0.325	-
Artificial Sea Water	186.7	0.306	-	223	0.311	-	217.4	0.307	-
End of Experiment									
	Ganf			Gatam			GANFg		
	Z-average (d-nm)	Pdl	Zeta potential (mV)	Z-average (d-nm)	Pdl	Zeta potential (mV)	Z-average (d-nm)	Pdl	Zeta potential (mV)
Stock Suspension	527.5	0.123	-15.9	389.4	0.164	-13	441.2	0.285	-14.8
<i>M. edulis Culture Media</i>	221.4	0.32	-	164.3	0.23	-	237.2	0.226	-
Artificial Sea Water	278.3	0.418	-	220.5	0.348	-	348.1	0.77	-

Table 2: DLS results measured in stock suspension, cell culture media and ASW at the start of the experiment and at the end. Zeta potential was only able to measured in the stock suspensions due to the high ionic strengths in the test media.

<i>Statistical Significance in gene expression: in vivo</i>									
	GANF			GATam			GANFg		
	0.01 mg/L	0.1 mg/L	1 mg/L	0.01 mg/L	0.1 mg/L	1 mg/L	0.01 mg/L	0.1 mg/L	1 mg/L
Cat	0.01	0.09	0.05	0.04	0.37	0.5	0.15	0.15	0.15
HSP70	0.13	0.13	0.5	0.06	0.15	0.15	0.15	0.15	0.06
GST	0.29	0.29	0.29	0.19	0.46	0.03	0.06	0.13	0.13
SOD	0.11	0.11	0.45	0.13	0.15	0.13	0.33	0.23	0.08
MT	0.37	0.37	0.06	0.15	0.06	0.15	0.01	0.03	0.1541
P53	0.15	0.15	0.06	0.15	0.06	0.15	0.01	0.15	0.01

PgP	0.01	0.33	0.16	0.21	0.05	0.19	0.11	0.41	0.01
CP450	0.05	0.5	0.5	0.37	0.32	0.32	0.29	0.29	0.06
Asyn	0.03	0.15	0.01	0.15	0.06	0.15	0.01	0.07	0.07
Lys	0.33	0.33	0.33	0.15	0.06	0.15	0.16	0.29	0.04
Na.K	0.08	0.25	0.23	0.15	0.06	0.15	0.15	0.15	0.13
MRP	0.43	0.45	0.43	0.04	0.41	0.04	0.41	0.32	0.03
Btub	0.15	0.06	0.02	0.15	0.06	0.015	0.15	0.15	0.06

Table 3: P-values, measured through Kruskal-Wallis and Dunn, of *M. edulis* hemocytes exposed *in vivo*. Stars indicate p-values <0.05 with + indicating a up regulation and – indicating down regulation.

<i>Statistical Significant in gene expression: in vitro</i>									
	GANF			GATam			GANFg		
	0.01 mg/L	0.1 mg/L	1 mg/L	0.01 mg/L	0.1 mg/L	1 mg/L	0.01 mg/L	0.1 mg/L	1 mg/L
Cat	+0.37	+0.37	+0.37	0.27	0.323	0.17	0.21	0.21	0.21
HSP70	-0.03*	-0.15	-0.03*	0.15	0.03*	0.01*	0.01*	0.13	0.01*
GST	-0.15	-0.03	-0.01*	0.15	0.01*	0.10	0.01*	0.15	0.01*
SOD	-0.09	-0.07	-0.01*	0.01*	0.02*	0.15	0.01*	0.01*	0.15
MT	-0.15	-0.03*	-0.01*	0.06	0.06	0.01*	0.04*	0.13	0.01*
Lys	0.06	0.15	0.15	0.16	0.29	0.04	0.15	0.15	0.08
PgP	+0.33	+0.33	+0.03*	0.21	0.08	0.19	0.06	0.15	0.15
CP450	-0.33	+0.16	-0.16	0.11	0.11	0.25	0.29	0.19	0.19
Asyn	+0.13	+0.13	+0.13	0.09	0.21	0.01*	0.01*	0.15	0.03*
Btub	-0.11	-0.05*	-0.01*	0.01*	0.02*	0.15	0.07	0.07	0.01*
Na.K	-0.15	-0.03*	-0.01*	0.15	0.02*	0.01*	0.15	0.15	0.08
P53	+0.13	+0.13	-0.15	0.01	0.07	0.37	0.06	0.15	0.15

MRP	+0.33	-0.16	+0.16	0.33	0.16	0.16	0.04*	0.16	0.29
------------	-------	-------	-------	------	------	------	--------------	------	------

Table 4: P-values, measured through Kruskal-Wallis and Dunn, of *M. edulis* hemocytes exposed *in vitro*.

Stars indicate p-values <0.05 with + indicating a up regulation and – indicating down regulation.

VIP Values						
	GAtam (in vivo)	GAtam (in vitro)	GANFg (in vivo)	GANFg (in vitro)	GANF (in vitro)	GANF (in vivo)
Asyn	1.06	0.97	1.34	0.94	0.95	1.43
P53	1.05	1.13	1.34	1.14	0.97	1.3
MT	1.09	1	1.4	1.02	0.89	1.28
PgP	1.16	1.01	0.93	1.02	0.67	1.06
HSP70	0.94	1.01	1.08	0.92	0.94	1.03
B.Tub	0.92	1.17	0.93	0.98	0.96	1.03
SOD	0.82	1.16	0.84	1.49	0.97	0.98
Na.K	0.97	1.01	0.84	0.51	0.87	0.98
Cat	1.39	0.72	0.33	0.82	0.28	0.92
CP450	0.78	0.88	0.62	1.16	0.61	0.9
Lys	1.3	0.96	0.82	1.06	1.8	0.6
GST	0.65	1.07	0.85	1.04	1.21	0.53
MRP	0.6	0.8	1.04	0.12	0.95	0.4

Table 5: VIP values of genes expression for each exposure condition to CNFs. VIP values below 0.8 were removed from the analysis.

Correlation with I _D /I _G -band ratio						
	0.01 mg/L		0.1 mg/L		1 mg/L	
	<i>in vitro</i>	<i>in vivo</i>	<i>in vitro</i>	<i>in vivo</i>	<i>in vitro</i>	<i>in vivo</i>
Cat	0.52	0.06	-0.16	-0.44	0.56	0.51
HSP70	-0.93*	0.84*	-0.3	0.26	0.32	0.23
GST	-0.91*	0.69*	0.7*	0.59	-0.22	0.49
SOD	-0.55	0.85*	-0.74*	0.55	0.79*	0.57
MT	-0.88*	0.54	-0.07	0.42	0.48	0.77*
Lys	-0.07	0.30	-0.92*	0.12	0.83*	0.86*
PgP	0.69	-0.36	-0.93*	0.32	-0.29	0.94*
CP450	0.46	-0.39	-0.94*	0.3	0.84*	0.66
Asyn	-0.97*	0.87*	-0.29	0.29	0.78*	0.89*
Btub	-0.62	1*	-0.65	0.21	-0.18	0.51

Nak	0.94*	0.53	0.9*	0.19	0.32	0.39
P53	-0.34	0.15	0.96*	0.26	0.34	0.89*
MRP	0.75*	0.5	0.06	0.82*	0.45	0.97*

Table 6: Table showing the correlation between the D/G-band ratio, measured through Raman spectroscopy, and gene expression. *Indicates statistical significant (P<0.05) with + indicating a positive relationship with purity and – indicating a negative relationship with purity.

Correlation with Reported CNF Purity						
	0.01 mg/L		0.1 mg/L		1 mg/L	
	<i>in vitro</i>	<i>in vivo</i>	<i>in vitro</i>	<i>in vivo</i>	<i>in vitro</i>	<i>in vivo</i>
Cat	-0.66	0.28	0.47	0.75*	-0.2	-0.58
HSP70	0.57	-0.33	-0.35	-0.79*	-0.76*	0.39
GST	0.74*	-0.23	-0.92*	-0.65	0.70*	0.13
SOD	-0.02	-0.35	0.23	-0.92*	-0.21	0.02
MT	0.67	-0.34	-0.12	0.22	0.1	-0.26
Lys	-0.52	-0.37	0.64	0.5	-0.33	-0.38
PgP	-0.89*	-0.27	0.58	0.32	0.8*	-0.54
CP450	-0.73*	-0.03	0.68*	0.16	-0.54	-0.43
Asyn	0.64	-0.39	-0.30	0.36	-0.3	-0.43
Btub	0.03	-0.83*	0.06	-0.76*	0.64	0.11
Nak	-0.85*	-0.93*	-0.84*	-0.74*	-0.69*	0.23
P53	0.82*	-0.69*	-0.64	0.39	0.05	-0.5
MRP	-0.84*	-0.11	-0.57	-0.77*	0.04	-0.78*

Table 7: Table showing the correlation between carbon nanofiber purity and gene expression. *indicate statistical significant (P<0.05) with + indicating a positive relationship with purity and – indicating a negative relationship with purity.

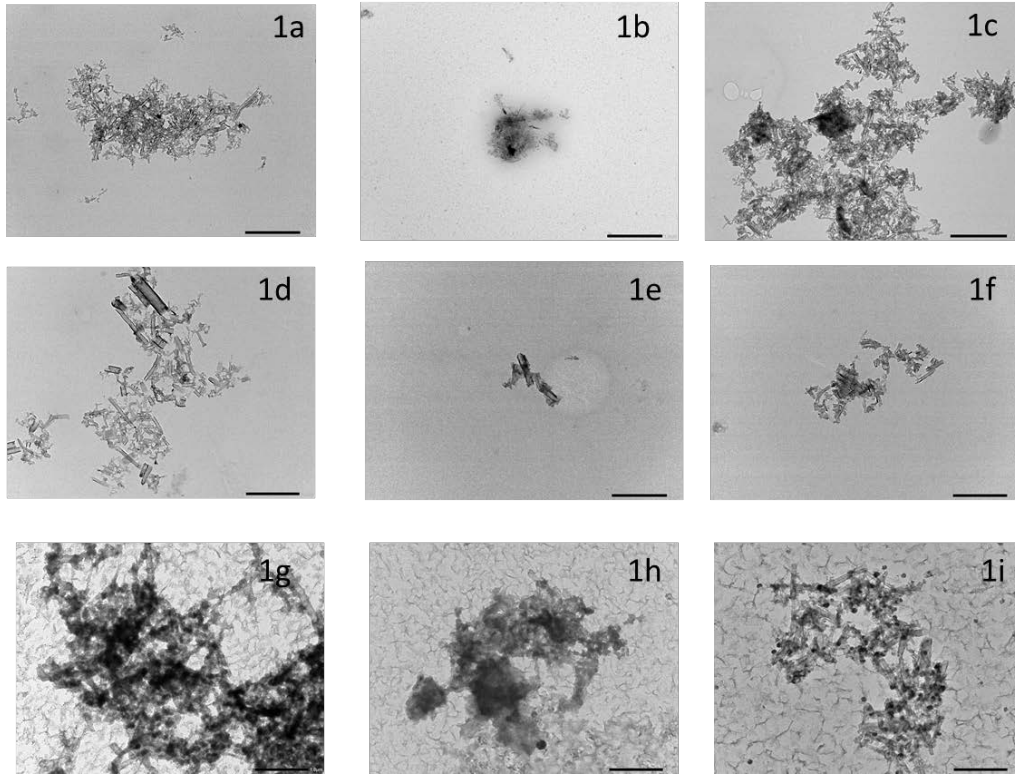


Figure 1a-i: TEM images of GANF (1a), GATam (1b) and GANFg (1c) prepared in stock suspensions compared with GANF (1d), GATam (1e) and GANFg (1f) in culture media and GANF (1g), GATam (1h) and GANFg (1i) prepared in ASW. Black bars indicate 1 μ m.

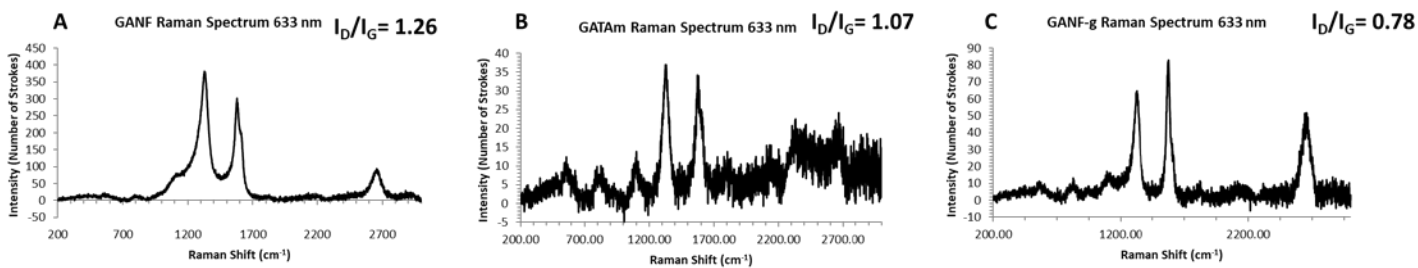


Figure 2a-c: Raman spectra of carbon nanofibers are expressed as a function of intensity in relation to the raman shift with peaks representing the D-band and G-band. To measure the structural purity of

GANF (A), GATam (B) and GANFg (C) the ratio of intensity between the D-band and G-band (I_D/I_G) is used.

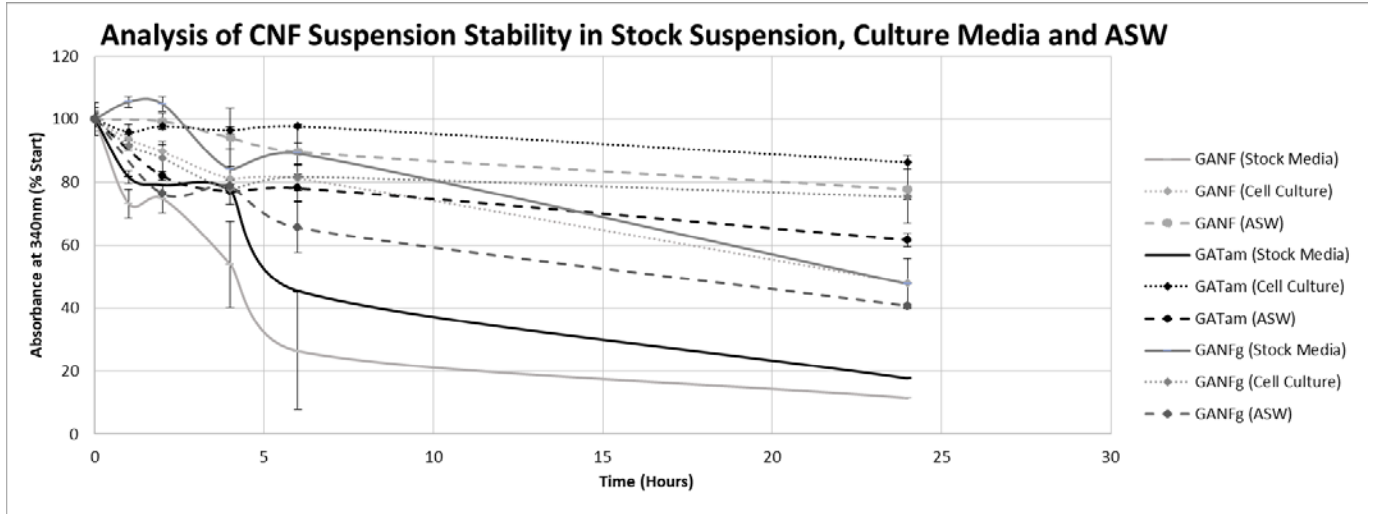


Figure 3: Optical density (340nm) as an approximation of suspension stability of the CNFs in the stock suspensions, cell culture media and in ASW over 24 hours.

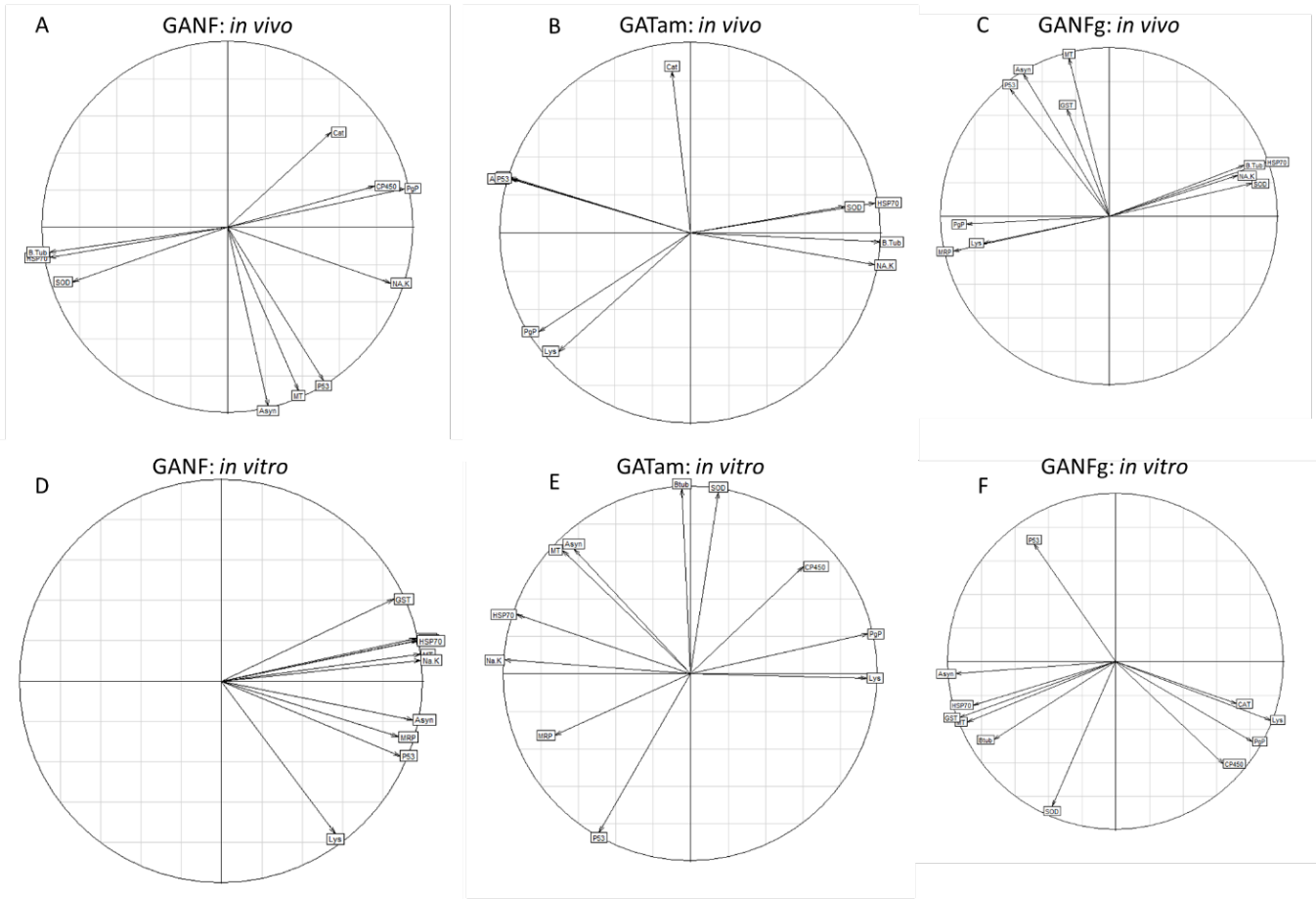


Figure 4: PLS-DA correlation for all test conditions *in vivo* for GANF (A), GATam (B) and GANFg (C) as well as *in vitro* for GANF (D), GATam (E) and GANFg (F) plotted on a factorial plane. Orientation of the vectors describes how strongly each gene describes the axes as well as the relationship between genes.

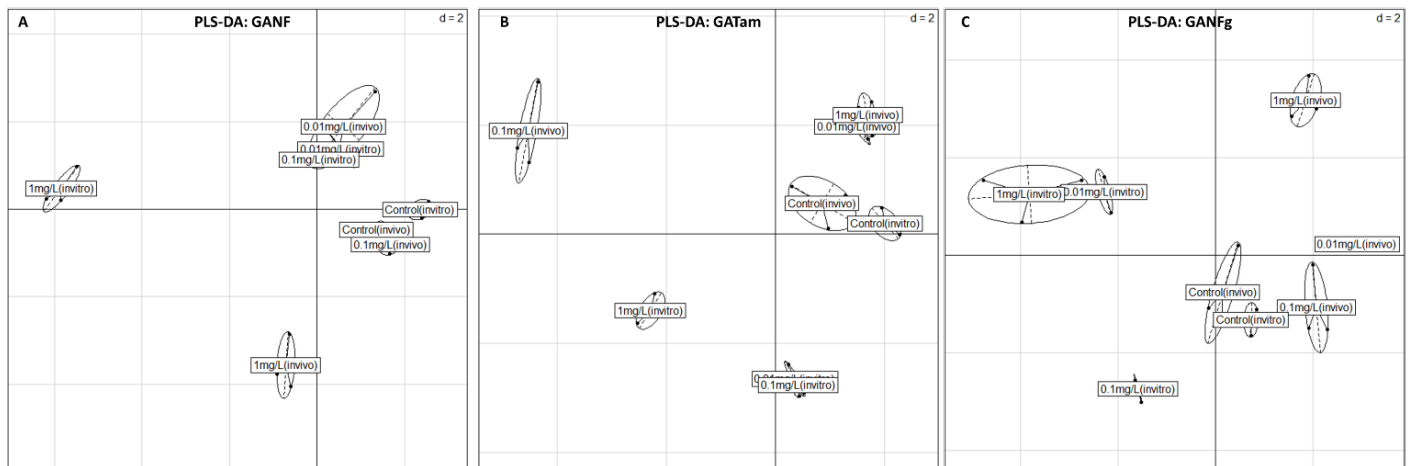


Figure 5: PLS-DA analysis of *M. edulis* hemocytes exposed *in vitro* and *in vivo* to GANF (A), GAtam (B) and GANFg (C) at 0.01, 0.1 and 1mg.L⁻¹.